NATIONAL ADVISORY COMMITTEE FOR AERONAUTICS

REPORT No. 769

THE EFFECT OF MASS DISTRIBUTION ON THE LATERAL STABILITY AND CONTROL CHARACTERISTICS OF AN AIRPLANE AS DETERMINED BY TESTS OF A MODEL IN THE FREE-FLIGHT TUNNEL

By JOHN P. CAMPBELL and CHARLES L. SEACORD, Jr.

1943

For sale by the Superintendent of Documents, U. S. Government Printing Office, Washington 25, D. C. - - - - - - - - - - Price 15 cents

AERONAUTIC SYMBOLS

1. FUNDAMENTAL AND DERIVED UNITS

	Symbol	Metric		English	
		Unit	Abbreviation	Unit	Abbreviation
Length	l	meter	m	foot (or mile)	ft (or mi)
Time	t	second	s	second (or hour)	sec (or hr)
Force	F	weight of 1 kilogram	kg	weight of 1 pound	lb
Power	P	horsepower (metric)		horsepower	hp
Speed	V	kilometers per hour	kph	miles per hour	mph
		meters per second	mps	feet per second	fps

2. GENERAL SYMBOLS

W Weight$=mg$

g Standard acceleration of gravity$=9.80665$ m/s^2 or 32.1740 ft/sec^2

m Mass$=\frac{W}{g}$

I Moment of inertia$=mk^2$. (Indicate axis of radius of gyration k by proper subscript.)

μ Coefficient of viscosity

ν Kinematic viscosity

ρ Density (mass per unit volume)

Standard density of dry air, 0.12497 kg-m^{-4}-s^2 at 15° C and 760 mm; or 0.002378 lb-ft^{-4} sec^2

Specific weight of "standard" air, 1.2255 kg/m^3 or 0.07651 lb/cu ft

3. AERODYNAMIC SYMBOLS

S Area

S_w Area of wing

G Gap

b Span

c Chord

A Aspect ratio, $\frac{b^2}{S}$

V True air speed

q Dynamic pressure, $\frac{1}{2}\rho V^2$

L Lift, absolute coefficient $C_L=\frac{L}{qS}$

D Drag, absolute coefficient $C_D=\frac{D}{qS}$

D_0 Profile drag, absolute coefficient $C_{D0}=\frac{D_0}{qS}$

D_i Induced drag, absolute coefficient $C_{Di}=\frac{D_i}{qS}$

D_p Parasite drag, absolute coefficient $C_{Dp}=\frac{D_p}{qS}$

C Cross-wind force, absolute coefficient $C_C=\frac{C}{qS}$

i_w Angle of setting of wings (relative to thrust line)

i_t Angle of stabilizer setting (relative to thrust line)

Q Resultant moment

Ω Resultant angular velocity

R Reynolds number, $\rho\frac{Vl}{\mu}$ where l is a linear dimension (e.g., for an airfoil of 1.0 ft chord, 100 mph, standard pressure at 15° C, the corresponding Reynolds number is 935,400; or for an airfoil of 1.0 m chord, 100 mps, the corresponding Reynolds number is 6,865,000)

α Angle of attack

ϵ Angle of downwash

α_0 Angle of attack, infinite aspect ratio

α_i Angle of attack, induced

α_a Angle of attack, absolute (measured from zero-lift position)

γ Flight-path angle

REPORT No. 769

THE EFFECT OF MASS DISTRIBUTION ON THE LATERAL STABILITY AND CONTROL CHARACTERISTICS OF AN AIRPLANE AS DETERMINED BY TESTS OF A MODEL IN THE FREE-FLIGHT TUNNEL

By JOHN P. CAMPBELL and CHARLES L. SEACORD, Jr.

Langley Memorial Aeronautical Laboratory
Langley Field, Va.

National Advisory Committee for Aeronautics

Headquarters, 1500 New Hampshire Avenue NW., Washington 25, D. C.

Created by act of Congress approved March 3, 1915, for the supervision and direction of the scientific study of the problems of flight (U. S. Code, title 49, sec. 241). Its membership was increased to 15 by act approved March 2, 1929. The members are appointed by the President, and serve as such without compensation.

REPORT No. 769

THE EFFECT OF MASS DISTRIBUTION ON THE LATERAL STABILITY AND CONTROL CHARACTERISTICS OF AN AIRPLANE AS DETERMINED BY TESTS OF A MODEL IN THE FREE-FLIGHT TUNNEL

By JOHN P. CAMPBELL and CHARLES L. SEACORD, Jr.

SUMMARY

The effects of mass distribution on lateral stability and control characteristics of an airplane have been determined by flight tests of a model in the NACA free-flight tunnel. In the investigation, the rolling and yawing moments of inertia were increased from normal values to values up to five times normal. For each moment-of-inertia condition, combinations of dihedral and vertical-tail area representing a variety of airplane configurations were tested.

The results of the flight tests of the model were correlated with calculated stability and control characteristics and, in general, good agreement was obtained. The tests showed the following effects of increased rolling and yawing moments of inertia: no appreciable change in spiral stability; reductions in oscillatory stability that were serious at high values of dihedral; a reduction in the sensitivity of the model to gust disturbances; and a reduction in rolling acceleration provided by the ailerons, which caused a marked increase in time to reach a given angle of bank. The general flight behavior of the model became worse with increasing moments of inertia but, with combinations of small effective dihedral and large vertical-tail area, satisfactory flight characteristics were obtained at all moment-of-inertia conditions.

INTRODUCTION

A recent trend in design has been to distribute weight along the wings of an airplane instead of concentrating it in the fuselage. This redistribution of weight, which has been brought about largely by changes from single-engine to twin-engine design and by the increased use of wing guns and wing fuel tanks, has resulted in greater rolling and yawing moments of inertia for the airplane and has thereby increased the difficulty of obtaining satisfactory lateral stability. Because of this trend, theoretical investigations (references 1 and 2) have recently been made to determine the effects of large increases in moments of inertia on lateral stability. The results of these investigations indicated that the range of values of dihedral and vertical-tail area for satisfactory oscillatory stability becomes progressively smaller with increasing moments of inertia.

In order to verify experimentally the results of such theoretical investigations and to determine the effects of the indicated stability changes on general flight behavior, an investigation has been carried out in the NACA free-flight tunnel with a 1/10-scale, free-flying dynamic model loaded to represent a wide range of values of rolling and yawing moments of inertia. For each moment-of-inertia condition, a range of dihedral angles and vertical-tail areas that represented a variety of airplane configurations was covered.

Calculations were made to determine the theoretical stability and control characteristics of the particular model tested in order that the results obtained by theory and experiment could be correlated.

SYMBOLS

k_X	radius of gyration about X-axis, feet
k_Z	radius of gyration about Z-axis, feet
I_X	moment of inertia about X-axis, slug-feet^2 (mk_X^2)
I_Z	moment of inertia about Z-axis, slug-feet^2 (mk_Z^2)
m	mass, slugs
C_L	lift coefficient (L/qS)
C_Y	lateral-force coefficient (Y/qS)
C_n	yawing-moment coefficient $\left(\frac{\text{Yawing moment}}{qbS}\right)$
C_l	rolling-moment coefficient $\left(\frac{\text{Rolling moment}}{qbS}\right)$
L	lift, pounds
Y	lateral force, pounds
q	dynamic pressure, pounds per square foot $\left(\frac{1}{2}\rho V^2\right)$
b	wing span, feet
c	wing chord, feet
S	wing area, square feet
C_{n_β}	rate of change of yawing-moment coefficient with angle of sideslip, per radian ($\partial C_n/\partial\beta$)
C_{l_β}	rate of change of rolling-moment coefficient with angle of sideslip, per radian ($\partial C_l/\partial\beta$)
C_{Y_β}	rate of change of lateral-force coefficient with angle of sideslip, per radian ($\partial C_Y/\partial\beta$)
C_{n_r}	rate of change of yawing-moment coefficient with yawing velocity, per unit of $rb/2V$ $\left(\partial C_n \Big/ \partial \frac{rb}{2V}\right)$
C_{n_p}	rate of change of yawing-moment coefficient with rolling velocity, per unit of $pb/2V$ $\left(\partial C_n \Big/ \partial \frac{pb}{2V}\right)$
C_{l_p}	rate of change of rolling-moment coefficient with rolling velocity, per unit of $pb/2V$ $\left(\partial C_l \Big/ \partial \frac{pb}{2V}\right)$
C_{l_r}	rate of change of rolling-moment coefficient with yawing velocity, per unit of $rb/2V$ $\left(\partial C_l \Big/ \partial \frac{rb}{2V}\right)$

743430—47

β angle of sideslip, radians
r yawing angular velocity, radians per second
V airspeed, feet per second
p rolling angular velocity, radians or degrees per second
ρ air density, slugs per cubic foot
P period of lateral oscillation, seconds
t time, seconds
ϕ angle of bank, degrees
ψ angle of yaw, degrees
δ_f flap deflection, degrees
R Routh's discriminant
D, E coefficients in stability quartic equation, given in reference 1

APPARATUS

The investigation was carried out in the NACA free-flight tunnel, which is equipped for testing free-flying dynamic airplane models. A complete description of the tunnel and its operation is given in reference 3. Force tests made to determine the static lateral-stability derivatives were run on the free-flight-tunnel six-component balance described in reference 4. A photograph of the test section of the tunnel showing a model in flight is given as figure 1.

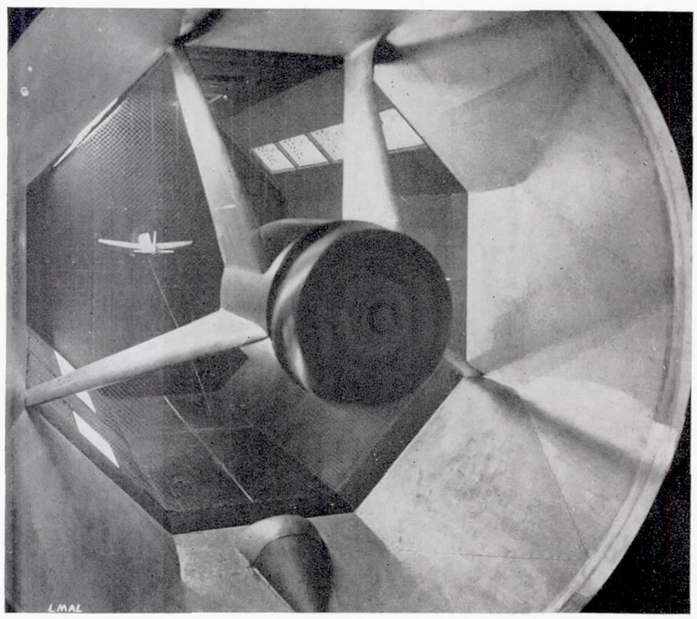

FIGURE 1.—Test section of NACA free-flight tunnel showing powered model in flight.

A three-view drawing of the model used in the tests is shown in figure 2, and photographs of the model are presented in figures 3 and 4. The 1/10-scale model, which in over-all dimensions represented a modern fighter airplane, was constructed principally of balsa and was equipped with movable control surfaces similar to those described in references 3 and 4. For all tests, the model was equipped with a split flap 60 percent of the wing span and 25 percent of the wing chord. The flap was deflected 60°.

The rolling and yawing moments of inertia of the model were varied by shifting lead weights from the fuselage to the wing tips. The effective dihedral was changed by altering the geometric dihedral angle of the outer panel, as indicated in figure 2. Four geometrically similar vertical tails (fig. 2) were used on the model to produce changes in vertical-tail area.

METHODS

STABILITY AND CONTROL CALCULATIONS

Boundaries for neutral spiral stability ($E=0$), neutral oscillatory stability ($R=0$), and neutral directional stability ($D=0$) were calculated for all moment-of-inertia conditions by means of the stability equations of reference 5 with the addition of the terms including product of inertia. It was assumed in the calculations that the angle between the principal longitudinal axis of inertia and the flight path was 5°, which was the angle of attack of the model in the flight tests. Values of the static lateral-stability derivatives, C_{n_β}, C_{l_β}, and C_{Y_β}, used in the calculations were obtained from force tests of the model. The value of the rotary derivative C_{n_r} was obtained from free-oscillation tests of the model in the free-flight tunnel (reference 6); whereas, the other rotary derivatives, C_{n_p}, C_{l_p}, and C_{l_r}, were estimated from the charts of reference 7 and from the formulas of reference 1. Values of the stability derivatives used in the calculations are given in table I. All the calculated boundaries are shown on the stability chart of figure 5.

The period of the lateral oscillation was calculated for some conditions by use of formula (21) given in reference 5.

TABLE I.—VALUES OF STABILITY DERIVATIVES USED IN COMPUTATIONS

[C_{l_β} is a dependent variable]

C_{Y_β}	C_{n_β}	C_{l_p}	C_{n_p}	C_{l_r}	C_{n_r}
−0.196	−0.0040	−0.47	−0.0520	0.2530	−0.0472
−.201	−.0022	−.47	−.0517	.2533	−.0484
−.226	.0065	−.47	−.0503	.2547	−.0545
−.326	.0415	−.47	−.0431	.2619	−.0790
−.426	.0765	−.47	−.0336	.2714	−.1035
−.526	.1115	−.47	−.0217	.2833	−.1280
−.626	.1465	−.47	−.0070	.2980	−.1525

The banking motions of the model following abrupt aileron maneuvers with different moments of inertia were calculated for a condition of small positive dihedral and large vertical-tail area. For these calculations the method of reference 8 was used and the model was assumed to have freedom only in roll.

TESTING PROCEDURE

The model was flown at each test condition and its stability and control characteristics were noted by the pilot. In addition, motion-picture records were made of some flights in order to supplement the pilot's observations with quantitative stability and control data.

The spiral stability of the model was determined by visual observation during sideslips across the tunnel with controls fixed. Increasing inward sideslip was taken as an indication of spiral instability.

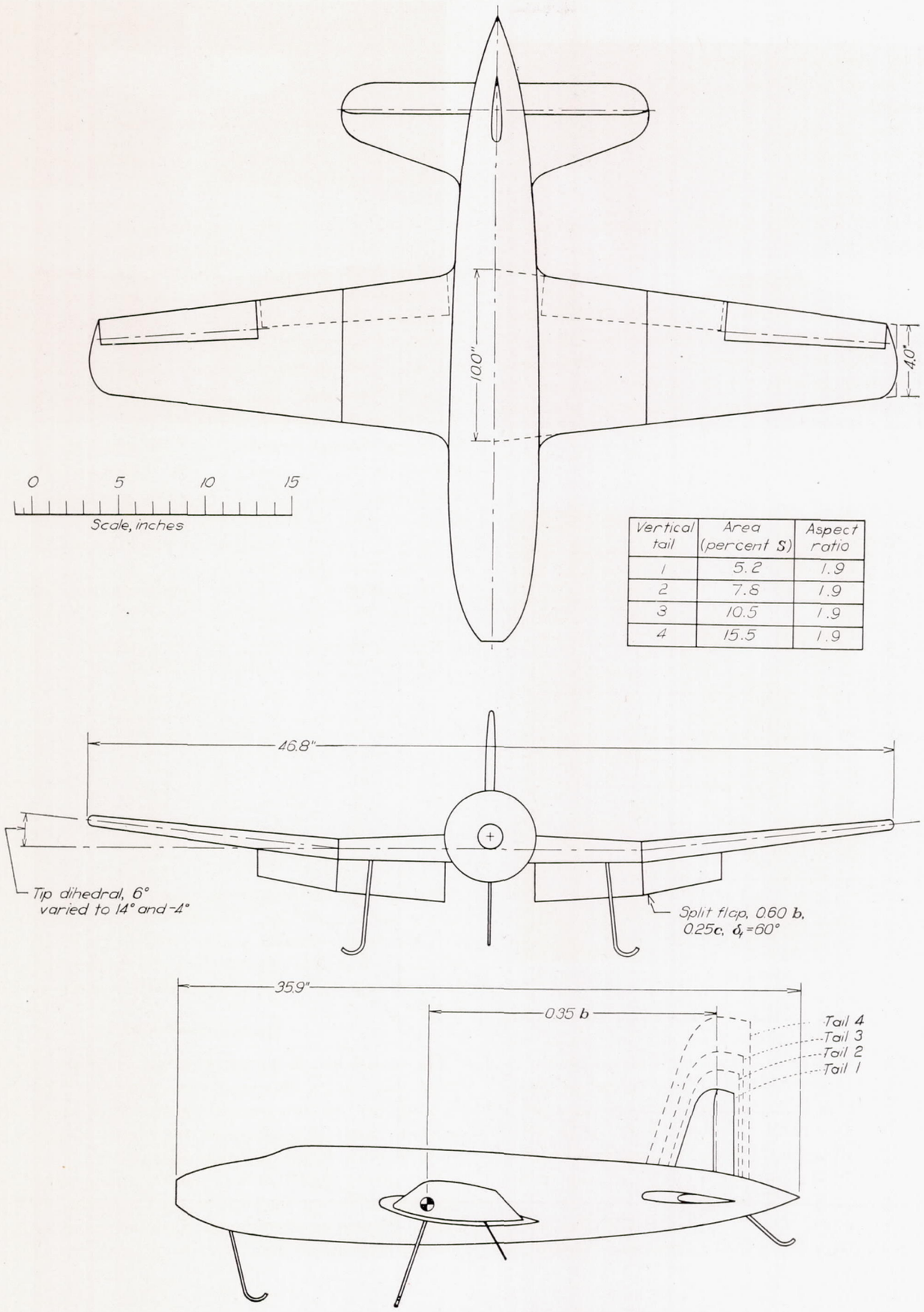

Vertical tail	Area (percent S)	Aspect ratio
1	5.2	1.9
2	7.8	1.9
3	10.5	1.9
4	15.5	1.9

FIGURE 2.—Drawing of model used in free-flight-tunnel mass-distribution investigation.

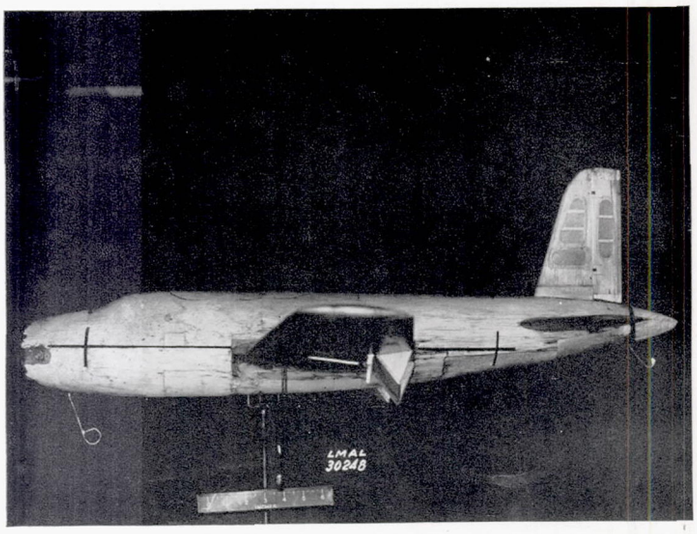

FIGURE 3.—Side view of model used in mass-distribution investigation in the NACA free-flight tunnel.

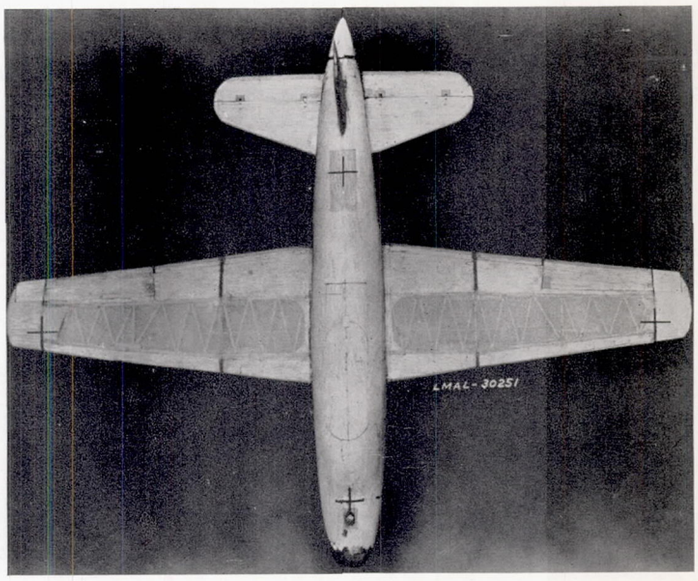

FIGURE 4.—Plan view of model used in mass-distribution investigation in the NACA free-flight tunnel.

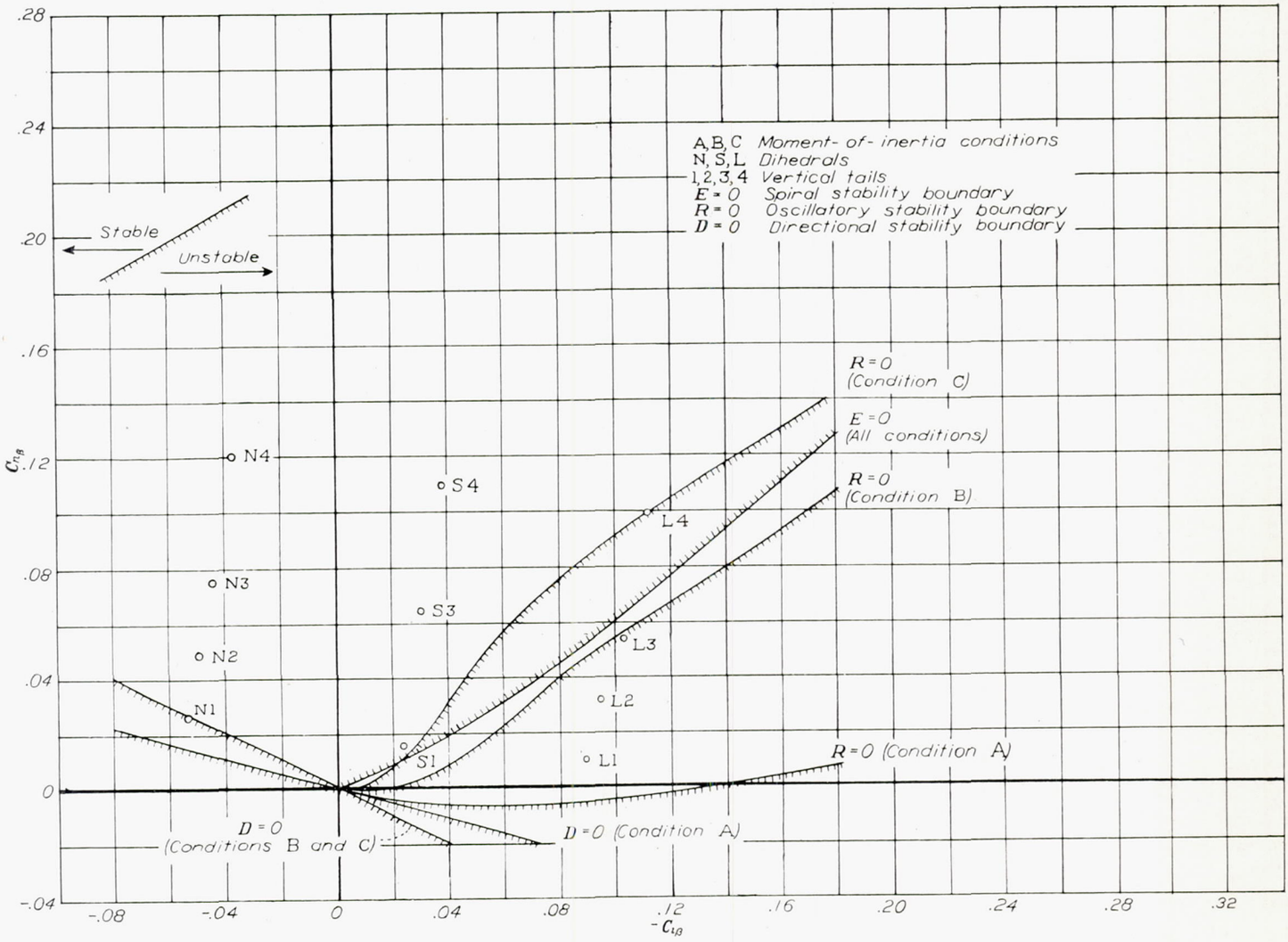

FIGURE 5.—Stability chart showing stability boundaries and model configurations. C_L=1.0 for all boundaries and configurations.

General oscillatory stability characteristics with controls fixed were noted by the pilot, and the damping and period of the lateral oscillations after abrupt rudder deflections were recorded by the cameras for each test condition.

The directional stability was judged by the yawing behavior of the model after gust disturbances and by the amount of adverse yawing produced by aileron control.

The steadiness, or the reaction of the model to the normal gustiness in the air stream, was noted for all test conditions. This characteristic was apparently not very closely related to other stability characteristics and was therefore judged independently.

The effectiveness of the ailerons in rolling the model was noted by the pilot and was measured from camera records of abrupt aileron maneuvers. The effect of adverse yawing on aileron control for the various test conditions was determined by visual observation.

Throughout the investigation, an effort was made to determine the best combinations of dihedral and vertical-tail area for each moment-of-inertia condition and to establish on the lateral stability chart ($-C_{l_\beta}$ against C_{n_β}) the boundaries between regions of satisfactory and unsatisfactory flight behavior. Flight-behavior ratings based on the pilot's opinion of the general stability and control characteristics of the model were recorded for each test condition. Although the accuracy of these ratings depended upon the pilot's ability to recognize unsatisfactory conditions, it is believed that the ratings give a true indication of the effect of changes in the variables involved because each rating was based on a number of separate flights.

RANGE OF VARIABLES

The parameters varied during the investigation were rolling and yawing moments of inertia, effective dihedral $-C_{l_\beta}$, and effective vertical-tail area C_{n_β}. The weight of the model was held constant to simulate an airplane wing loading of 30 pounds per square foot. All the tests were made at an airspeed of 51 feet per second, which corresponded to a lift coefficient of 1.0.

Because the rolling and yawing moments of inertia were changed by varying the radii of gyration, k_X and k_Z, while the weight was held constant, the inertia changes in this investigation are expressed in terms of k_X/b and k_Z/b. These ratios or their reciprocals are the conventional nondimensional expressions for radii of gyration in stability calculations.

In making the moment-of-inertia changes, k_X/b and k_Z/b were varied in such a manner that the value of $\left(\frac{k_Z}{b}\right)^2-\left(\frac{k_X}{b}\right)^2$ remained constant. Changing the moments of inertia in this way corresponds to changing the proportion of weight carried in the wings. In the tests with high values of k_X/b and k_Z/b, the model therefore represented an airplane with such loads as guns, ammunition, and fuel tanks installed in the wings instead of the fuselage.

Three moment-of-inertia conditions were tested corresponding to the values of k_X/b and k_Z/b in the following table, in which the relative values of moments of inertia are also given in order to afford a better indication of the magnitude of the inertia changes:

Condition	k_X/b	$\frac{I_X}{I_X \text{ (Condition A)}}$	k_Z/b	$\frac{I_Z}{I_Z \text{ (Condition A)}}$
A	0.127	1.00	0.197	1.00
B	.200	2.49	.247	1.57
C	.286	5.08	.322	2.67

These moment-of-inertia conditions are represented on the graph of k_X/b against k_Z/b in figure 6 by the points A, B, and C. Condition A is intended to simulate an average mass distribution for modern single-engine fighter airplanes. Condition B represents the probable upper limit of moments of inertia for present-day conventional airplanes. Condition C represents the extremely high values of the parameters k_X/b and k_Z/b that result in the case of airplanes with very small span or with exceptionally large loads in the wings. Condition C very nearly simulates the moments of inertia of a flying wing with uniform spanwise mass distribution.

In order to illustrate the trend of present-day airplanes toward higher moments of inertia, various other points are also plotted in figure 6. The squares connected by arrows show this trend in successive models of single-engine fighter airplanes of the same design. The triangles represent mass distributions of several modern twin-engine and multiengine designs.

An example is given in figure 6 to show the effect on moments of inertia of adding large bombs or extra fuel tanks to the wings of a typical fighter airplane. The position of the mass distribution of this airplane on the plot is changed from Y to Z by the addition of a 2000-pound bomb or fuel tank midway out on each wing. It is evident that an installation of this kind substantially increases the rolling and yawing moments of inertia.

Three values of dihedral were used in the tests: a large positive dihedral, a small positive dihedral, and a moderate negative dihedral, which are represented by the symbols L, S, and N, respectively. The value of C_{l_β} for each dihedral varied slightly with vertical-tail area, as shown in figure 5. The four vertical tails used in the tests and designated by the numbers 1, 2, 3, and 4 (fig. 2) provided a range of C_{n_β} from 0.01 to 0.12. Exact values of C_{n_β} and C_{l_β} for each model configuration were determined by force tests of the model and are shown in figure 5.

The various configurations are represented by combinations of symbols, for convenience and brevity; for example, condition S3B has small positive dihedral S, vertical tail 3, and moment-of-inertia condition B.

RESULTS AND DISCUSSION

SPIRAL STABILITY

The spiral stability of the model was not affected by changes in moments of inertia. The flight tests agreed with theory in this respect for, as indicated in figure 5, the theoretical spiral stability boundary is not changed by variation of k_X/b and k_Z/b. Ratings for spiral stability for the various model configurations are presented in figure 7.

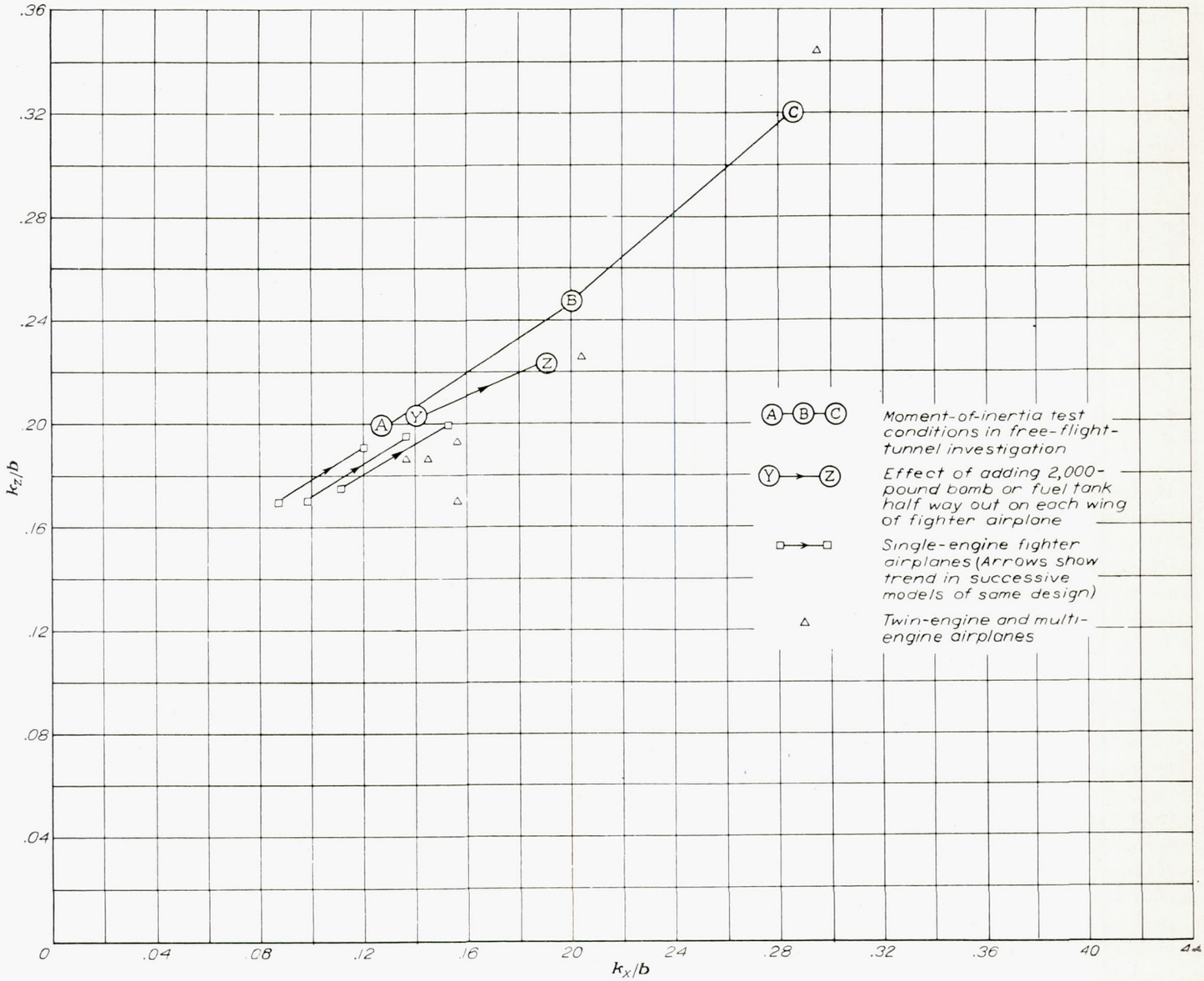

FIGURE 6.—Range of values of $\frac{k_x}{b}$ and $\frac{k_z}{b}$ covered in investigation.

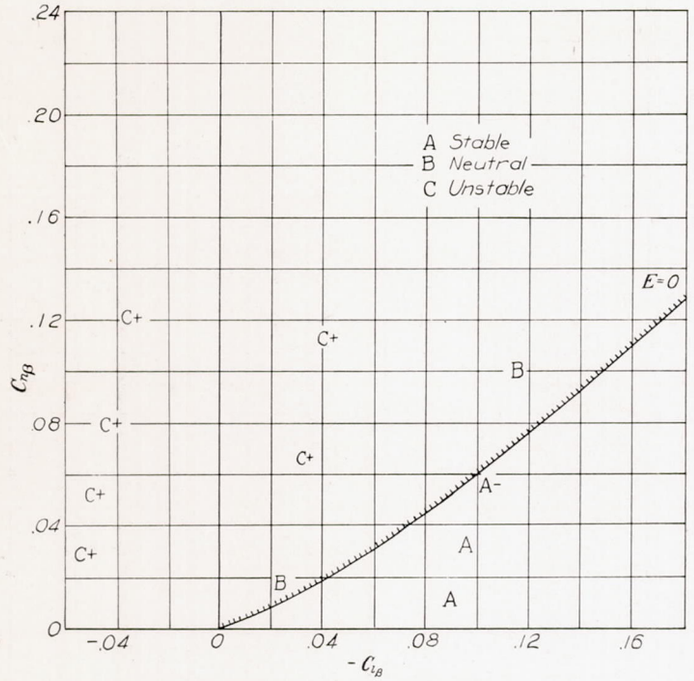

FIGURE 7.—Spiral-stability ratings for different model configurations. C_L=1.0. (Average ratings for all moment-of-inertia conditions.)

It was interesting to note that, for the negative dihedral condition, increasing the moments of inertia did not materially increase the difficulty of flying the model. It might be expected that, because of the spiral instability with negative dihedral, increasing the rolling moment of inertia, and consequently reducing the rolling acceleration produced by the ailerons, would cause difficulty in recovering from a banked attitude. Such was not the case, however, probably because the acceleration of the dropping wing after a gust disturbance was also smaller with the increased inertia. At times this reduced rolling acceleration even caused an apparent improvement in spiral stability because the model seemed to diverge more slowly following a gust disturbance.

The flight-test results emphasized the fact that, for the range of conditions tested, spiral instability has virtually no significance in determining general flight characteristics. It can be seen from figure 7 that the model was spirally unstable with both the small positive and the negative dihedrals. Yet even with the negative dihedral, no rapid spiral divergence was noted and the model was not appreciably harder to fly than with the large positive dihedral.

OSCILLATORY STABILITY

Increasing the moments of inertia definitely reduced the oscillatory stability of the model and for some model configurations introduced conditions of dangerous oscillatory instability. The data of figure 8 show graphically the changes in the damping of the lateral oscillation with change in mass distribution for various combinations of dihedral and vertical-tail area. Inasmuch as an accurate quantitative measure of the damping could not be obtained for all conditions, the results are presented in the form of qualitative ratings for damping at each condition. The approximate quantitative equivalents of these ratings are:

Rating	Qualitative rating	Approximate quantitative equivalent
A	Stable	Damps to ½ amplitude in less than 2 cycles
B	Slightly stable	Damps to ½ amplitude in 2 cycles or more
C	Neutral	Zero damping
D	Slightly unstable	Builds up to double amplitude in more than 1 cycle
E	Dangerously unstable	Builds up to double amplitude in 1 cycle or less

A comparison of the theoretical oscillatory stability boundaries (R=0) in figure 8 with the ratings for damping of the oscillation obtained in the flight tests of the model indicates good agreement between theory and flight results.

Figure 9 shows that increasing the moments of inertia caused an increase in the period of the lateral oscillation, as indicated by theory. The experimentally determined values for the period were slightly smaller than the calculated values.

The ratings in figure 8 show that, although increasing the moments of inertia reduced the oscillatory stability for virtually all model configurations, the magnitude of the reduction varied greatly for the different combinations of dihedral and vertical-tail area. In general, the effects of moment of inertia on the oscillation damping were more pronounced with the large dihedral and the small vertical-tail areas. This variation in the magnitude of inertia effects with model configuration was in good agreement with the variation indicated by the shifting of the theoretical oscillatory stability boundaries shown on the stability charts ($-C_{l_\beta}$ against C_{n_β}) in figure 8. With increasing moments of inertia the boundaries move upward and inward on the charts and thereby show the greatest inertia effects at large values of $-C_{l_\beta}$ and small values of C_{n_β}. It appears both from these boundary shifts and from the flight ratings for oscillation damping that a complete picture of the effects of increased moments of inertia on oscillatory stability can be obtained only by an analysis of the effects over a wide range of model configurations.

Small positive dihedral.—With the small positive dihedral, the effect of increased moments of inertia on oscillatory stability was relatively small for all values of vertical-tail area. Even for the condition of least oscillatory damping with this dihedral (condition S1C), no unstable oscillations were noted although the damping was very light. With the two largest vertical tails (tails 3 and 4) and the small dihedral, the oscillatory stability for conditions B and C, though less than that for condition A, was considered satisfactory.

Large positive dihedral.—With the large positive dihedral, increasing the moments of inertia caused pronounced reductions in oscillatory stability for all values of vertical-tail area. Conditions of dangerous oscillatory instability were encountered with the smallest tail (tail 1) at loading condition B and with all tails except the largest (tail 4) at loading condition C. These unstable conditions were considered dangerous because sustained flights were impossible as a result of oscillations that increased in amplitude despite intensive efforts of the pilot to control the model.

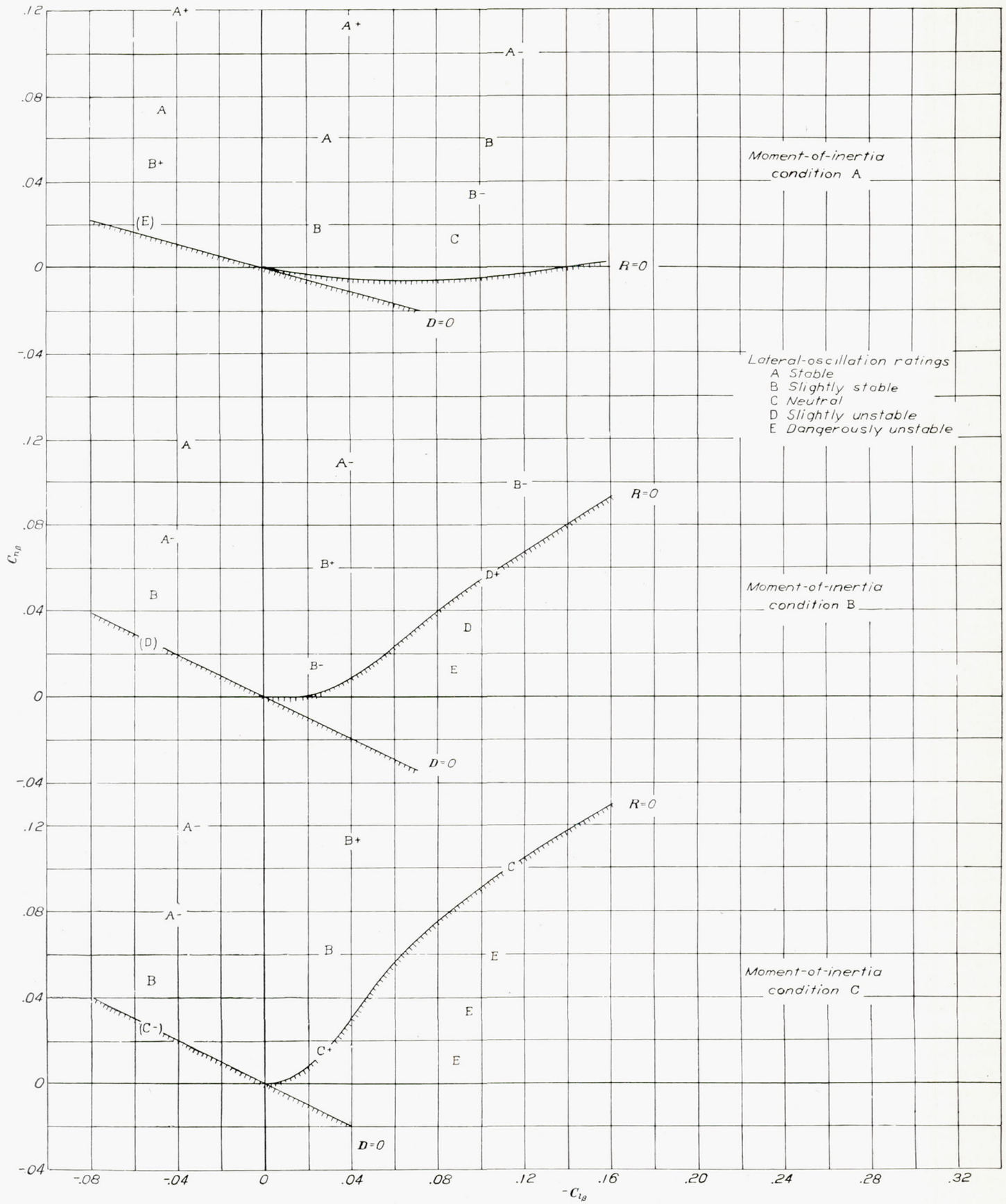

FIGURE 8.—Ratings for damping of lateral oscillation for different test conditions. C_L=1.0. (Ratings possibly influenced by directional stability enclosed in parentheses.)

For some conditions, such as L3B and L4C, unstable oscillations were encountered in flights with controls fixed, but these oscillations could be terminated at will by control applications and were therefore not considered particularly dangerous.

The pronounced effect of moments of inertia on oscillatory stability with the large positive dihedral is illustrated graphically in figure 10 by photographically recorded time histories of flights at conditions L3A, L3B, and L3C. The two upper sets of curves in figure 10 are records of the lateral oscillations with controls fixed, which were started by abrupt rudder deflections. A comparison of the curves shows that changing from moment-of-inertia condition A to moment-of-inertia condition B caused the model to become oscillatorily unstable in flights with controls fixed. As pointed out in the preceding paragraph, however, this instability was not especially dangerous when the lateral controls were used properly.

The two lower sets of curves in figure 10 show that increasing the moments of inertia from condition A to condition C produced an unstable oscillation that could not be stopped by aileron and rudder control. At condition L3C, the oscillation not only continued to build up despite aileron-control movements but also was of such strength that its period was not appreciably altered by the control applications. The flights at this condition, of course, were of very short duration and were usually terminated by an abrupt sideslip to the floor of the tunnel after the model had attained a very steep angle of bank. The motion-picture record for condition L3A, which is in sharp contrast with that of condition L3C, shows the positive and almost instantaneous effect of the ailerons in returning the model to level flight with normal moments of inertia and serves to emphasize the magnitude of the instability that effectively nullified the aileron control at condition L3C. The apparently unstable yawing motion shown in the record of condition L3A was probably caused by the fact that the rudder control applied simultaneously with the aileron control used to bank the model was not always of the required magnitude nor in the proper direction for returning the model to unyawed flight.

Negative dihedral.—With the negative dihedral, the effects of moment of inertia on oscillatory stability were less than with the positive dihedrals and were small for all values of vertical-tail area. With this dihedral, the lateral oscillation appeared to have a satisfactory rate of damping for all conditions except with the smallest tail (tail 1). A peculiar and sometimes violent form of instability was encountered at conditions N1A, N1B, and N1C. The instability, which appeared to be more directional than oscillatory in nature, was usually evidenced by yawing motions that increased in magnitude even when the ailerons and the rudder were used for control. In some flights at this unstable condition, the model yawed to a large angle and then rolled off abruptly with the leading wing going down. It was interesting to note that the flight behavior of the model with the negative

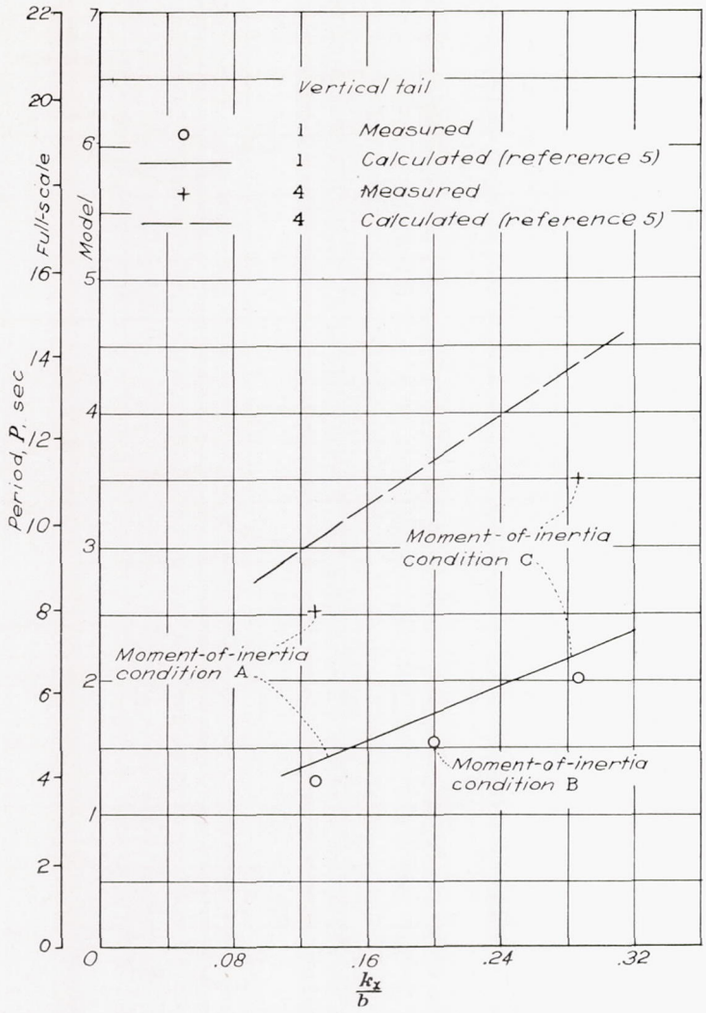

FIGURE 9.—Effect of moments of inertia on period of lateral oscillation. Small positive dihedral. C_L=1.0.

dihedral and tail 1 improved with increasing moments of inertia. This surprising effect appeared to be a direct result of slower, and therefore more easily controlled, yawing motions of the model with the higher moments of inertia.

The ratings for damping of the oscillation in figure 8 for conditions N1A, N1B, and N1C are given in parentheses because of the uncertainty as to whether the instability was oscillatory or directional in nature. It should be noted that these conditions on the stability diagram fall very near the boundary for neutral directional stability (D=0). In the negative dihedral range, and in fact for all spirally unstable conditions, the R=0 boundary is not an indication of neutral oscillatory stability because E, one of the coefficients of the stability equation, is negative. An examination of the roots of the stability equations for several negative dihedral conditions, however, reveals that oscillatory stability theoretically exists well below the D=0 boundary. It appears, therefore, that over the negative dihedral range directional divergence will occur before oscillatory instability, as indicated by the flight tests of the model.

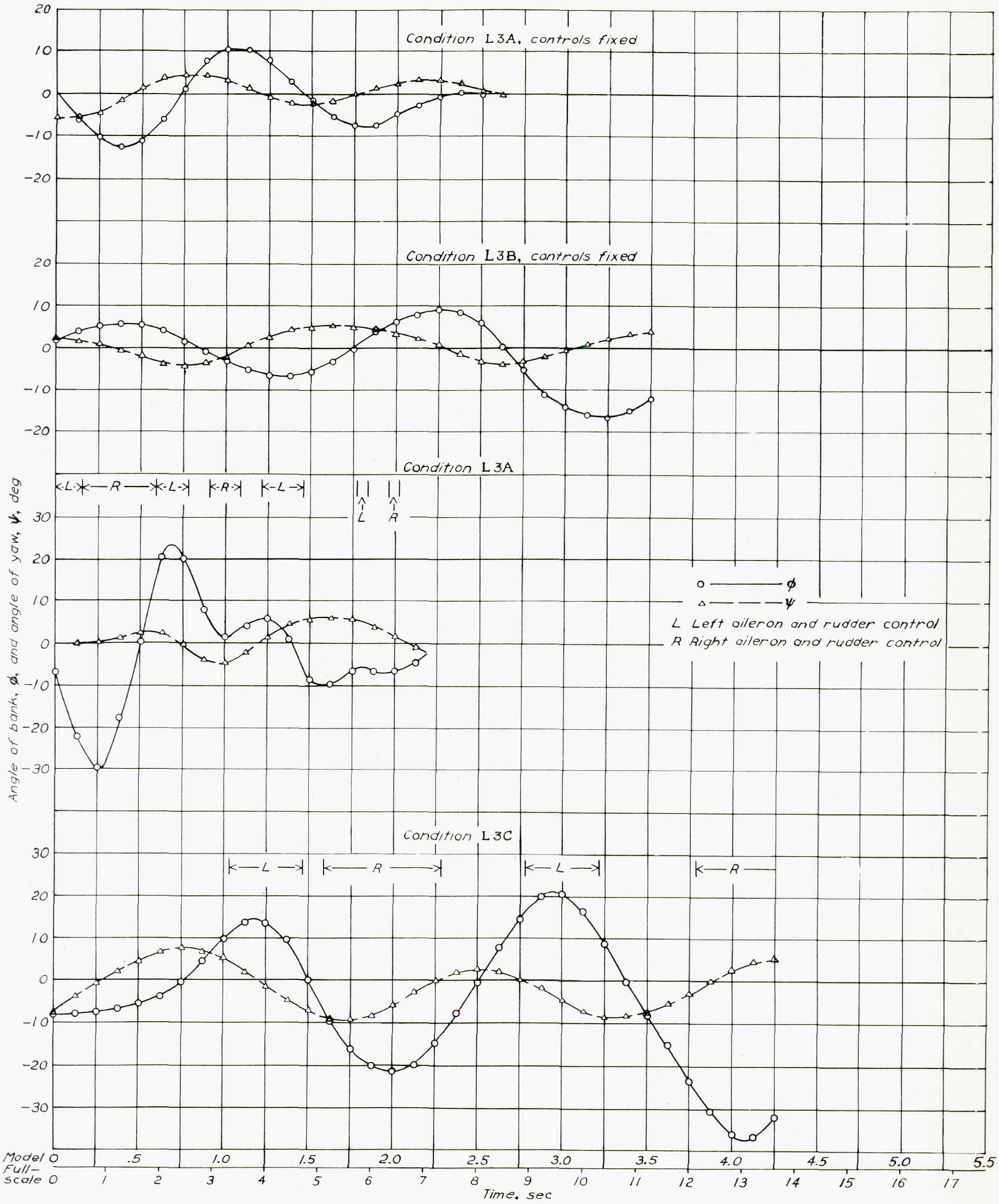

FIGURE 10.—Time histories of banking and yawing motions of model showing effect of increased moments of inertia on damping of lateral oscillation. Large positive dihedral. Vertical tail 3. C_L=1.0.

REACTION TO GUSTS

The reaction of the model to the normal gustiness in the air stream was improved by increasing the moments of inertia. With the high values of k_X/b and k_Z/b, the model was less sensitive to gust disturbances during smooth flight and appeared to be steadier both in roll and in yaw than with the lower moments of inertia. This effect, which was apparently purely inertial, was considered beneficial from a stability standpoint, but like some aerodynamic stabilizing effects was detrimental to lateral control, as will be shown in the following section.

It should be pointed out that the beneficial effects of high moments of inertia on the lateral steadiness of the model were present only during smooth flight. Once the smooth flight of the model was interrupted by a particularly violent gust or control disturbance, the high moments of inertia prolonged the effect of the disturbance and increased the difficulty of returning to steady flight.

LATERAL CONTROL

Increasing the moments of inertia caused marked increases in the time to reach a given angle of bank with aileron control. It is evident from the time histories of abrupt aileron maneuvers shown in figure 11 that this reduction was caused by decreased rolling acceleration The model accelerated so slowly during aileron maneuvers at conditions B and C that maximum rolling velocities could not be reached during the limited time and space available for the maneuvers.

Figure 11 shows that the test results were in excellent agreement with calculations of the pure banking motion of the model. These calculations, which were based on the assumption that the model had freedom only in roll, indicate that the maximum rolling velocity is not affected by changes in moments of inertia. Complete calculations of the banking motion of an airplane with three degrees of freedom (unpublished data) show, however, that increasing the moments of inertia reduces the final rolling velocity as well as the acceleration in roll. In any event, it appears that, with a very high rolling moment of inertia, the reduction in rolling acceleration alone is sufficient to lengthen noticeably the time required to attain a given angle of bank with aileron control.

The test data of figure 11 are made applicable to the airplane by additional scales for rolling velocity and time. By means of these scales, a better indication can be obtained of the effects of high moments of inertia on the angle of bank reached in a given time or on the time required to reach a given angle of bank for the full-scale airplane.

GENERAL FLIGHT BEHAVIOR

The general flight behavior became worse with increasing moments of inertia, as shown by the flight-behavior ratings in figure 12. It appeared that oscillatory stability was the predominant factor influencing the pilot's opinion of the general flight behavior, as is indicated by the similarity of the ratings on figures 8 and 12 for corresponding test conditions. The magnitude of the detrimental effects of increased inertia on general flight behavior, as on oscillatory stability,

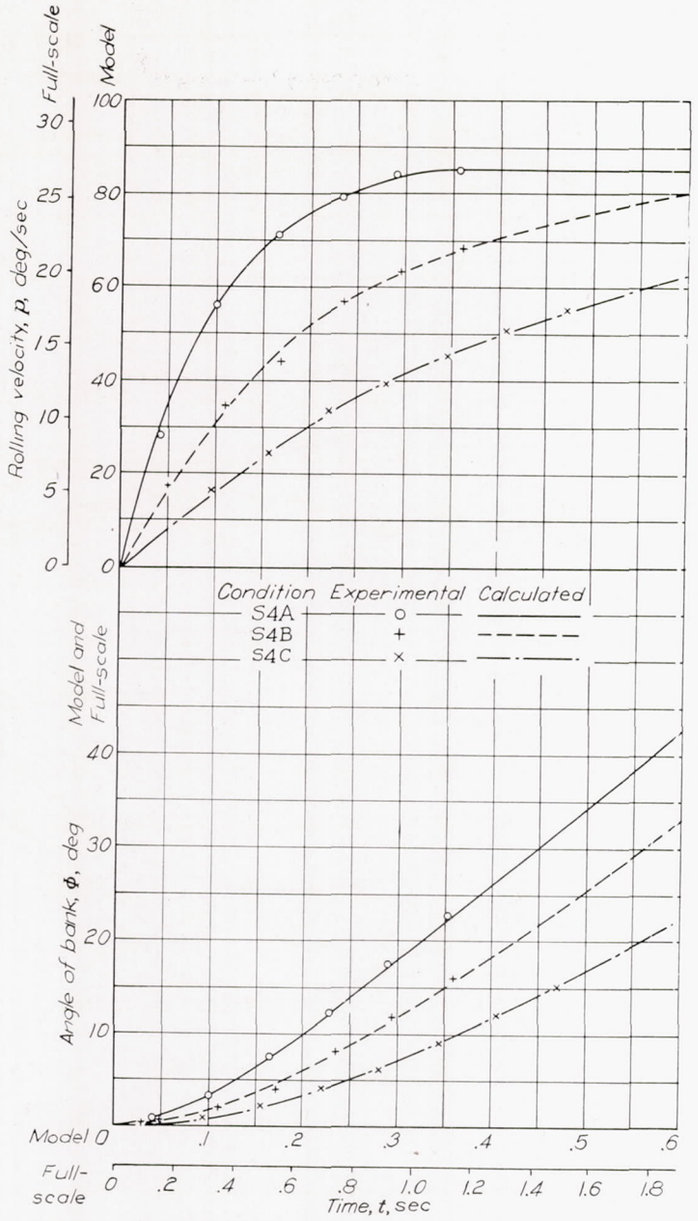

FIGURE 11.—Time histories of abrupt aileron maneuvers with different moment-of-inertia conditions. Small positive dihedral. Vertical tail 4. $C_L = 1.0$.

was dependent upon the model configuration; the greatest effects were observed with the large positive dihedral and the least effects were noted with the large vertical tails (tails 3 and 4) used in combination with the negative or small positive dihedrals.

Combinations of dihedral and vertical-tail area that gave satisfactory flight behavior at the different moment-of-inertia conditions are indicated in figure 12 by approximate boundaries that separate satisfactory and unsatisfactory regions on the stability charts. It is apparent from the manner in which the boundaries shift that the number of satisfactory combinations of dihedral and vertical-tail area decreased with increasing inertia. One model configuration (small positive dihedral and vertical tail 4), however, provided good general flight behavior for all moment-of-inertia conditions tested.

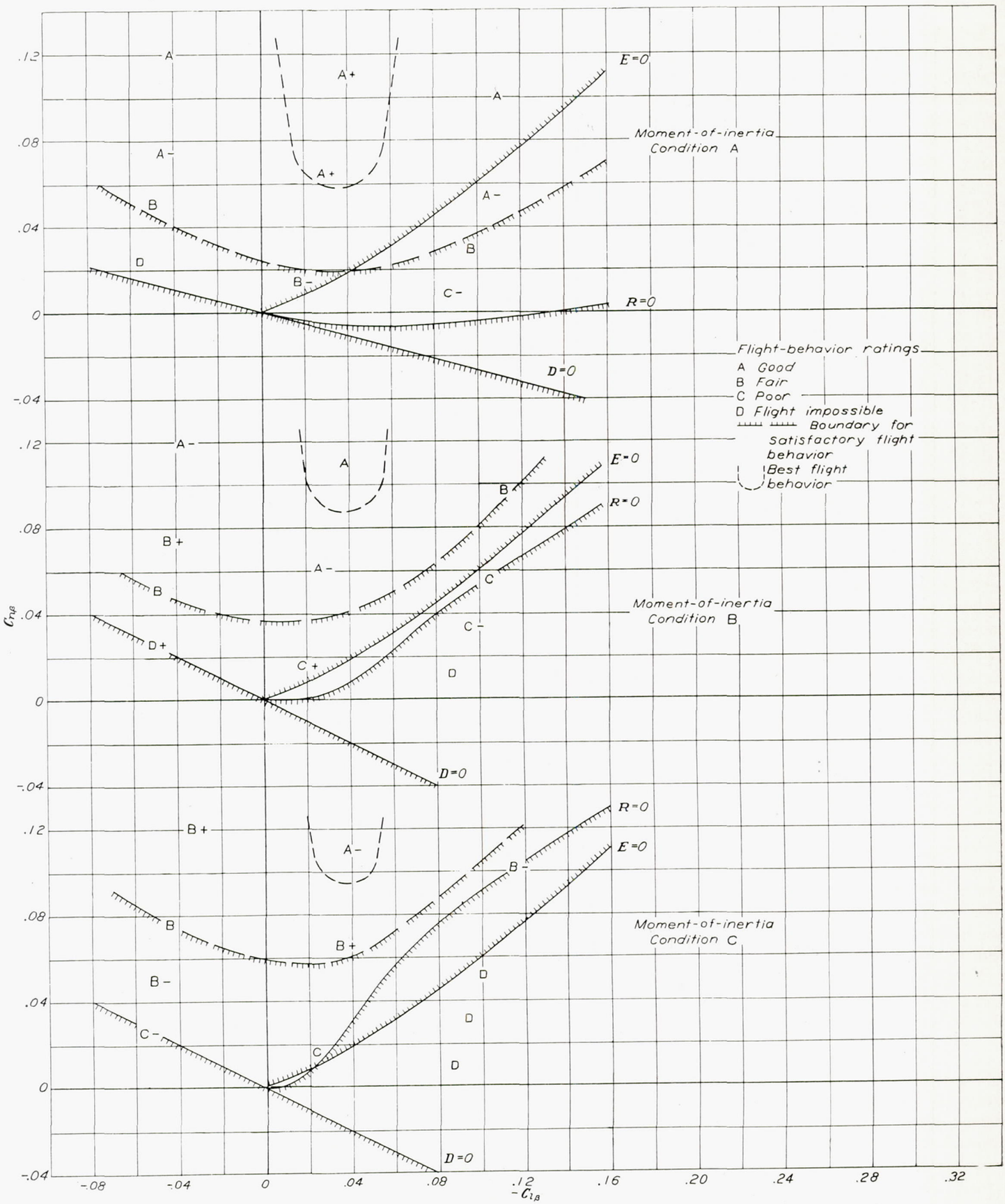

FIGURE 12.—Flight-behavior ratings for different test conditions. $C_L = .0$.

CONCLUSIONS

The effects of increased rolling and yawing moments of inertia on the lateral stability and control characteristics of an airplane as determined by tests of a model in the free-flight tunnel may be summarized as follows:

1. In general, the test results were in good agreement with theory in regard to the effects of moments of inertia on lateral stability and control.

2. Increasing the moments of inertia did not affect spiral stability and did not increase the difficulty of flying at a condition of spiral instability.

3. Increasing the moments of inertia reduced oscillatory stability. With negative or small positive dihedral the reduction in stability was not great even with the small vertical tails. With the large positive dihedral, however, large increases in the moments of inertia introduced dangerous oscillatory instability, especially with the smaller vertical tails.

4. With high moments of inertia, the model was less sensitive to gust disturbances and consequently flew more smoothly than with the normal moments of inertia.

5. Increasing the moments of inertia reduced the rolling acceleration provided by the ailerons and thereby caused a marked increase in the time required to attain a given angle of bank.

6. The general flight behavior became worse with increasing moments of inertia. The greatest effects of increased inertia were observed at conditions of large dihedral and small vertical-tail area.

7. Satisfactory flight characteristics for all moment-of-inertia conditions were obtained with the small dihedral ($C_{l_\beta}=-0.038$) and the large vertical tail area ($C_{n_\beta}=0.11$).

LANGLEY MEMORIAL AERONAUTICAL LABORATORY,
NATIONAL ADVISORY COMMITTEE FOR AERONAUTICS,
LANGLEY FIELD, VA., *July 20, 1943.*

REFERENCES

1. Bamber, Millard J.: Effect of Some Present-Day Airplane Design Trends on Requirements for Lateral Stability. NACA TN No. 814, 1941.
2. Bryant, L. W., and Pugsley, A. G.: The Lateral Stability of Highly Loaded Aeroplanes. R. & M. No. 1840, British A. R. C., 1938.
3. Shortal, Joseph A., and Osterhout, Clayton J.: Preliminary Stability and Control Tests in the NACA Free-Flight Wind Tunnel and Correlation with Full-Scale Flight Tests. NACA TN No. 810, 1941.
4. Shortal, Joseph A., and Draper, John W.: Free-Flight-Tunnel Investigation of the Effect of the Fuselage Length and the Aspect Ratio and Size of the Vertical Tail on Lateral Stability and Control. NACA ARR No. 3D17, 1943.
5. Zimmerman, Charles H.: An Analysis of Lateral Stability in Power-Off Flight with Charts for Use in Design. NACA Rep. No. 589, 1937.
6. Campbell, John P., and Mathews, Ward O.: Experimental Determination of the Yawing Moment Due to Yawing Contributed by the Wing, Fuselage, and Vertical Tail of a Midwing Airplane Model. NACA ARR No. 3F28, 1943.
7. Pearson, Henry A., and Jones, Robert T.: Theoretical Stability and Control Characteristics of Wings with Various Amounts of Taper and Twist. NACA Rep. No. 635, 1938.
8. Jones, Robert T.: A Simplified Application of the Method of Operators to the Calculation of Disturbed Motions of an Airplane. NACA Rep. No. 560, 1936.

U. S. GOVERNMENT PRINTING OFFICE: 1947

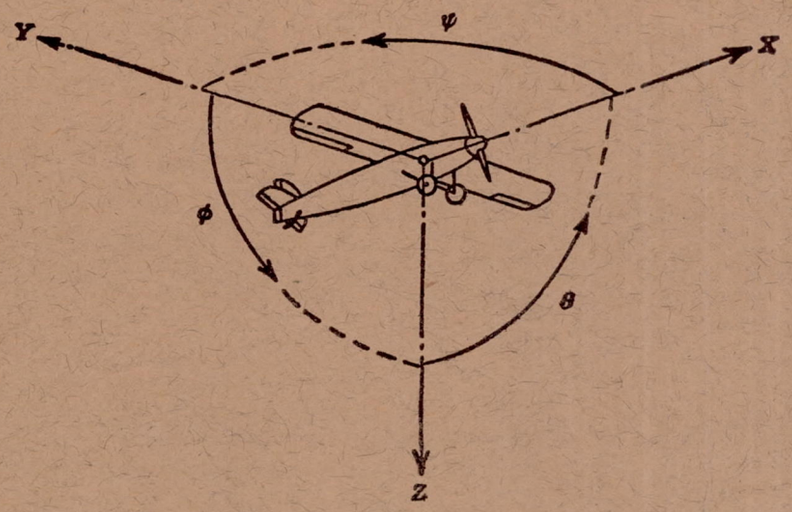

Positive directions of axes and angles (forces and moments) are shown by arrows

Axis		Force (parallel to axis) symbol	Moment about axis			Angle		Velocities	
Designation	Symbol		Designation	Symbol	Positive direction	Designation	Symbol	Linear (component along axis)	Angular
Longitudinal	X	X	Rolling	L	$Y \longrightarrow Z$	Roll	φ	u	p
Lateral	Y	Y	Pitching	M	$Z \longrightarrow X$	Pitch	θ	v	q
Normal	Z	Z	Yawing	N	$X \longrightarrow Y$	Yaw	ψ	w	r

Absolute coefficients of moment

$C_l = \frac{L}{qbS}$ (rolling) $\quad C_m = \frac{M}{qcS}$ (pitching) $\quad C_n = \frac{N}{qbS}$ (yawing)

Angle of set of control surface (relative to neutral position), δ. (Indicate surface by proper subscript.)

4. PROPELLER SYMBOLS

D Diameter

p Geometric pitch

p/D Pitch ratio

V' Inflow velocity

V_s Slipstream velocity

T Thrust, absolute coefficient $C_T = \frac{T}{\rho n^2 D^4}$

Q Torque, absolute coefficient $C_Q = \frac{Q}{\rho n^2 D^5}$

P Power, absolute coefficient $C_P = \frac{P}{\rho n^3 D^5}$

C_s Speed-power coefficient $= \sqrt[5]{\frac{\rho V^5}{P n^2}}$

η Efficiency

n Revolutions per second, rps

Φ Effective helix angle $= \tan^{-1}\left(\frac{V}{2\pi r n}\right)$

5. NUMERICAL RELATIONS

1 hp=76.04 kg-m/s=550 ft-lb/sec

1 metric horsepower=0.9863 hp

1 mph=0.4470 mps

1 mps=2.2369 mph

1 lb=0.4536 kg

1 kg=2.2046 lb

1 mi=1,609.35 m=5,280 ft

1 m=3.2808 ft